AGU PUBLICATIONS

Geophysical Research Letters

RESEARCH LETTER
10.1002/2015GL066726

Key Points:
- The unique character of plagioclase in lunar anorthosite supports the lunar magma ocean model
- At depths >70 km in the LMO, crystallizing anorthitic plagioclase may not show Na enrichment
- Sinking of hercynitic spinel yielded magmas with elevated Ab/An in spite of a Na-depleted Moon

Supporting Information:
- Supporting Information S1

Correspondence to:
H. Nekvasil,
Hanna.Nekvasil@stonybrook.edu

Citation:
Nekvasil, H., D. H. Lindsley, N. DiFrancesco, T. Catalano, A. E. Coraor, and B. Charlier (2015), Uncommon behavior of plagioclase and the ancient lunar crust, *Geophys. Res. Lett.*, *42*, 10,573–10,579, doi:10.1002/2015GL066726.

Received 23 OCT 2015
Accepted 2 DEC 2015
Accepted article online 11 DEC 2015
Published online 23 DEC 2015

Uncommon behavior of plagioclase and the ancient lunar crust

Hanna Nekvasil[1], Donald H. Lindsley[1], Nicholas DiFrancesco[1], Tristan Catalano[1], Aron E. Coraor[1], and Bernard Charlier[2]

[1]Department of Geosciences, State University of New York at Stony Brook, Stony Brook, New York, USA, [2]Department of Geology, University of Liege, Liege, Belgium

Abstract Calcic plagioclase, the dominant mineral of the anorthositic lunar crust, fails to show the Na enrichment during cooling that is typical of magmatic plagioclase. We show that this enigmatic behavior may arise during fractionation of highly calcic plagioclase at depths greater than ~70 km in the lunar magma ocean because of the development of a negative azeotropic configuration at high anorthite contents that impedes and may even reverse the standard plagioclase albite enrichment with dropping temperature. This result supports a high-pressure origin of this plagioclase consistent with the lunar magma ocean model. It also provides a new mechanism for forming lunar lithologies with sodic plagioclase from a highly Na-depleted Moon through gravitational settling of spinel and refines the compositional characteristics of the late stage residual liquids of the lunar magma ocean.

1. Introduction

The concept of a lunar magma ocean (LMO) emerged after the discovery of a plagioclase-rich (anorthositic) crust on the Moon [*Smith et al.*, 1970] and has been supported by the recognition of its global distribution from data from lunar meteorites [e.g., *Korotev et al.*, 2003], remote spectroscopy [e.g., *Hawke et al.*, 2003], and gravity field studies [e.g., *Besserer et al.*, 2014]. Formation of the anorthositic crust has been explained by flotation of highly calcic plagioclase and expulsion of trapped liquid by compaction and other processes [e.g., *Piskorz and Stevenson*, 2014] during the late stages of LMO crystallization (after approximately 80% crystallization) [*Snyder et al.*, 1992; *Elkins-Tanton et al.*, 2011], while dense ferromagnesian minerals accumulate on the floor of the LMO, forming the mantle [*Warren*, 1985]. As the only accessible lunar lithology attributed to the primary crystallization of the LMO, rocks of the ferroan anorthosite suite (FAS) play a vital role in providing information about the early differentiation of the Moon.

The crystallization behavior of plagioclase, the most abundant mineral in FAS rocks, has long been considered well understood, governed by the nearly ideal melting loop for plagioclase/silicate melt equilibria in the binary system Albite (Ab)-Anorthite (An) [*Bowen*, 1913] (Figure 1a) and in multicomponent systems [*Morse*, 2013]. All LMO crystallization models and proposed mechanisms for forming the secondary lithologies arising from post-LMO processes implicitly and explicitly incorporate this expected behavior of Na enrichment with decreasing temperature. However, FAS plagioclase does not show Ab enrichment. Instead, both individual crystals of plagioclase and FAS plagioclase grains as a group lie in a very restricted compositional region ($An_{94–98}$) [e.g., *Lindstrom and Lindstrom*, 1986; *Warren*, 1993; *Gross et al.*, 2014] in spite of the major compositional variation of coexisting solid solutions, specifically olivine and pyroxene (Figure 1b)—a variation that indicates a large temperature interval between the first saturation of plagioclase and the final solidus temperature. Compositional invariance occurs in plagioclase cumulate rocks on Earth and has been thought to arise from the inability of small amounts of interstitial melt to produce compositional evolution of a large amount of plagioclase during cooling [e.g., *Raedeke and McCallum*, 1980]. Such a restriction on compositional evolution may locally have played a role after lunar plagioclase accumulation; however, many FAS rocks have a significant fraction of nonplagioclase "liquid" component [*Warren*, 1990; *Namur et al.*, 2011]. Furthermore, formation of large amounts of nearly compositionally invariant plagioclase through ordinary processes would imply nearly isothermal conditions, conditions inconsistent with the large differences in Mg' of ferromagnesian minerals in different FAS units that suggest a wide temperature range of crystallization of anorthitic plagioclase. In this study, we investigated the possibility that restriction of Na enrichment is a primary crystallization feature unique to highly anorthitic plagioclase ($An \geq 94$) crystallizing at depth.

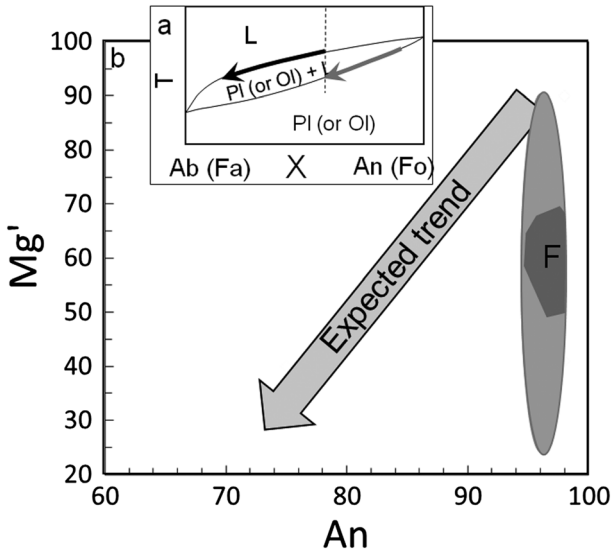

Figure 1. Expected versus observed plagioclase compositional evolution in the FAS rocks. (a) Melting loop that describes crystal/melt relations in the Ab-An (plagioclase) and Fo-Fa (olivine) systems. During cooling, minerals (gray arrow) and liquid (black arrow) become enriched in the component with the lower melting temperature. Dashed line is an arbitrary bulk composition. Symbols: L: liquid (silicate melt); Pl: plagioclase; and Ol: olivine. (b) Variation in Mg number [$Mg' = 100 \times Mg/(Mg + Fe^{2+})$] of low Ca ferromagnesian minerals with An content of plagioclase (mol%) in Apollo FAS rock samples (field F) [from *Papike et al*., 1997] and clasts from meteorites [*Goodrich et al*., 1984; *Gross et al*., 2014] (gray oval). The expected trend is based on the combination of the common melting loop topologies for both plagioclase and ferromagnesian minerals.

2. Complexities of Plagioclase Crystallization

Early experimental work on the melting relations of plagioclase in the binary system [*Lindsley*, 1969] demonstrated a change in calcic plagioclase/melt phase relations with pressure. Elevated pressure causes greater destabilization of crystalline anorthite relative to albite and, by approximately 1 GPa, induces saturation with the crystalline incongruent melting product corundum and development of a "pseudo"-negative azeotrope (Figure 2) (where the term pseudo indicates that unlike in the classic case, this topology lies within the field of stability of an incongruent melting product, namely, corundum here). This destabilization of anorthite and production of crystalline corundum (C) can be envisioned as resulting from a decrease in the activity of An component in the melt (a_{An}^{m}) due to dissociation as described by the homogeneous melt reaction

$$CaAl_2Si_2O_8{}^m = Al_2O_3{}^m + CaSiO_3{}^m + SiO_2{}^m \quad \text{(R1)}$$

and saturation with crystalline corundum once $\mu_{Al2O3(C)}{}^s = \mu_{Al2O3}{}^m$ (where μ_{Al2O3} is the chemical potential of Al_2O_3 in the solid (s) or melt (m)). This reaction models the structural dissociation noted in NMR studies of anorthite glass [*Stebbins and Xu*, 1997].

The topology of Figure 2 provides a mechanism to explain the lack of Ab enrichment in FAS plagioclase. For bulk compositions on the An side of the pseudoazeotrope, the effective An/(An + Ab) of the melt is greatly reduced because of reaction ((R1)) and the first-formed plagioclase is more albitic than the bulk composition (Figure 2a)—opposite to the common behavior (Figure 1a). Importantly, unlike for the melting loop or the classic azeotrope, in this pseudoazeotropic system, the plagioclase is more albitic than the combined composition of corundum + L (at the heavy black curve of Figure 2) but not more albitic than the L itself. Dropping temperature shifts reaction ((R1)) back to the left, causing a concomitant increase in activity of the An melt component and crystallization of increasingly calcic plagioclase. With decreasing pressure, reaction ((R1)) results in less dissociation and the pseudoazeotrope shifts closer to the An sideline (Figure 2b). This simple system also predicts the effect of fractionation; during fractionation of the more albitic plagioclase, the residual assemblage would show an increase in An/(An + Ab) and may stay to the An side of the pseudoazeotrope over much of a polybaric crystallization path. Countering this An enrichment during plagioclase fractionation is the effect of fractionation of corundum (or any aluminous phase arising incongruently). This will inhibit attainment of the original An/(An + Ab) ratio of the final assemblage and instead will push the residual assemblage to higher Ab/(Ab + An) ratios than the original bulk composition. The net result of fractionation of both phases would be plagioclase with composition that remains nearly invariant during crystallization. In contrast, plagioclase on the albite side of the pseudoazeotrope undergoes the standard evolution (Figure 1a) as does all plagioclase crystallizing at low pressures where there is no pseudoazeotrope. Fractionation of either or both crystallizing phases for such compositions would simply enhance the Ab enrichment of the final assemblage.

Although this topology holds great promise for explaining the anomalous compositional evolution of FAS plagioclase, three additional criteria must be met for it to be relevant to the LMO. First, the pseudoazeotrope

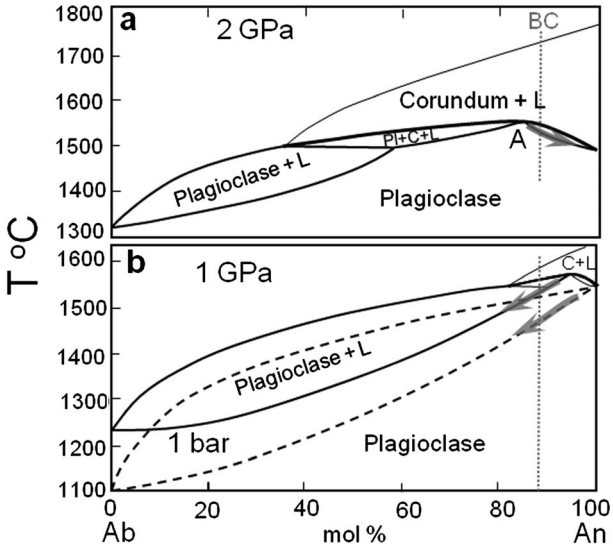

Figure 2. Phase relations in the plagioclase system. Phase relations based on experimental data of *Lindsley* [1969] at (a) 2 GPa and (b) 1 GPa, compared with the melting loop at 1 atm (dashed curves) [from *Bowen*, 1913]. A refers to the pseudoazeotrope. For the original bulk composition BC, the gray arrows show the compositional evolution of plagioclase with dropping temperature when plagioclase crystals are removed from contact with the melt (fractionated) during crystallization. Opposing this trend would be the effect of simultaneous loss of corundum (C) from the system. At 2 GPa, plagioclase undergoes mild Ca enrichment along the solidus curve; in contrast, at 1 GPa and 1 atm, it undergoes Na enrichment. The composition of the assemblage L + C in equilibrium with plagioclase lies along the heavy black boundary curves. Note the shift of the pseudoazeotrope to higher An contents with decreasing pressure.

must persist in multicomponent melts relevant to the differentiation of the LMO at plagioclase saturation. Second, since modeling constraints place plagioclase saturation at approximately 0.7 GPa in a 1000 km deep LMO [*Elkins-Tanton et al.*, 2011], the pseudoazeotrope must persist to shallower levels than in the simple system. Finally, the fact that only rocks with plagioclase compositions less albitic than ~An_{94} show anomalous behavior requires that the azeotrope must lie close to An_{94} at approximately 0.7 GPa.

Plagioclase in the LMO crystallized from a multicomponent melt containing olivine melt components [*Snyder et al.*, 1992; *Charlier et al.*, 2015]. Even at 1 bar, this permits the formation of an An melt component-consuming, homogeneous melt reaction that can be described by

$$2\,CaAl_2Si_2O_8{}^m + (Mg,Fe)_2SiO_4{}^m = 2\,(Mg,Fe)Al_2O_4{}^m + 2\,CaSiO_3{}^m + 3\,SiO_2{}^m \quad \text{(R2)}$$

which induces eventual saturation with hercynitic spinel $(Mg,Fe)Al_2O_4$ [*Osborn and Tait*, 1952]. Might the combined destabilization of anorthite melt component both with pressure and through reaction with olivine melt components be sufficient to stabilize the pseudoazeotrope to lower, LMO-relevant pressures? We evaluated this possibility through dynamic crystallization experiments at three pressures (0.35, 0.5, and 0.7 GPa). These experiments were designed to produce zoned crystals through first melting then cooling in successive sequences of controlled slow cooling followed by isothermal crystallization.

3. Experimental and Analytical Methods

3.1. Starting Materials

Starting materials for the two compositions investigated (on either side of the suspected pseudoazeotrope) $(An_{94}Ab_6)_{67}(Fo_{50}Fa_{50})_{33}$ and $(An_{90}Ab_{10})_{67}(Fo_{50}Fa_{50})_{33}$ were prepared by combining $Fo_{50}Fa_{50}$ composition (using SiO_2, MgO, Fe metal, and Fe_2O_3) with synthetic plagioclase crystals. Synthetic plagioclase was made by mixing stoichiometric quantities of SiO_2, Al_2O_3, $CaSiO_3$, and $Na_2Si_2O_5$ powders; loading this mixture into a platinum capsule; drying before welding the capsule shut; and heating to 1350°C for 10 days.

3.2. Procedure

Each mixture was loaded into graphite capsules. These were placed inside a graphite furnace with an exterior $BaCO_3$ sleeve (as per *Whitaker et al.* [2007]). All experiments began with cold, overpressurization of the sample by 0.2 GPa at room temperature (to ensure piston-out conditions); the sample was then brought to the melting temperature, and the pressure dropped to the final pressure. Samples were held at the melting temperature for 30 min for complete melting; then the temperature was decreased by 0.1°/min for 20° before being held constant for 10 h (allowing isothermal crystallization at the end of each cooling segment). The process was repeated until the final temperature was reached. This ensured the formation of zoned crystals that could be used to determine the compositional change during

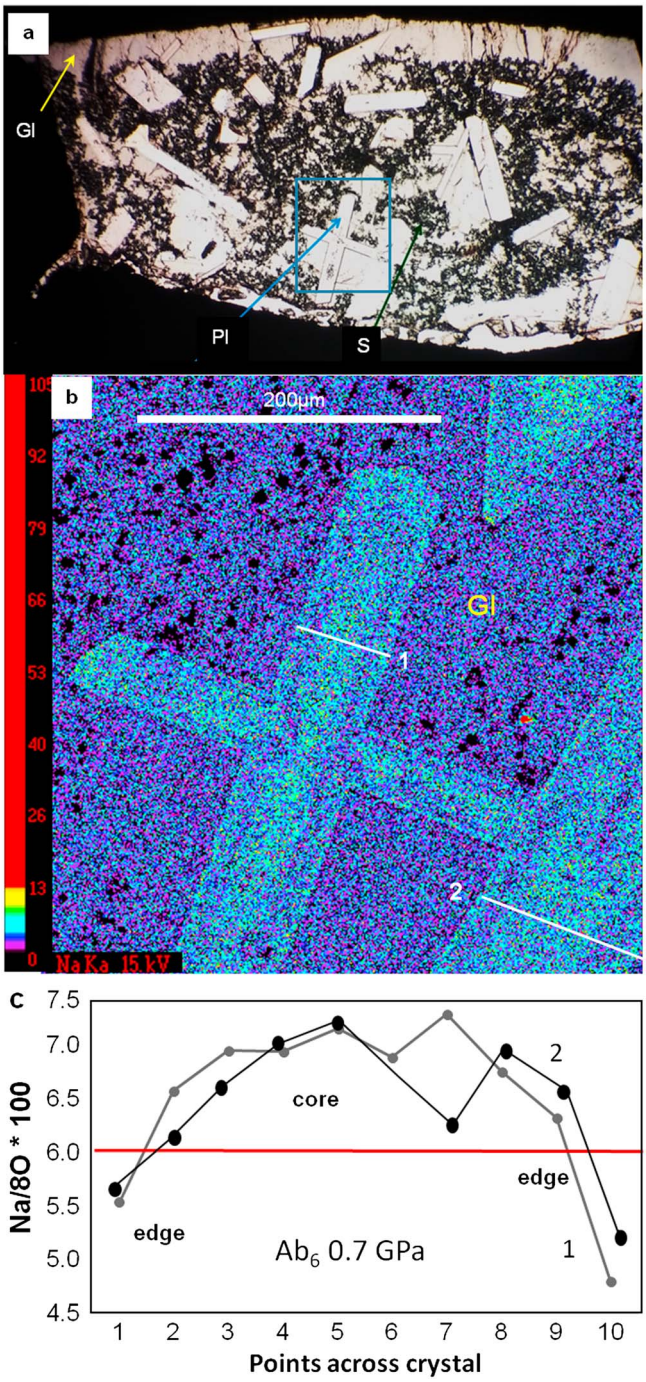

Figure 3. Characteristics of experimental products of dynamic cooling experiments at 0.7 GPa for the $(An_{94}Ab_6)_{67}(Fo_{50}Fa_{50})_{33}$ bulk composition. (a) Plane-polarized light photomicrograph. The graphite capsule (black) (oriented as for the experiment) surrounds the charge. Plagioclase grains (Pl) are the white euhedral crystals. The black grains are spinel (S). Note the clear glass (Gl) at the top and the gravitational settling of spinel to the bottom of the capsule. Region outlined in blue refers to the field of view of Figure 3b. The field of view is 4 mm. (b) Na X-ray maps of characteristic plagioclase crystals from electron microprobe analysis showing reverse zoning (cores that are more sodic than exterior zones) indicating that the bulk composition lies on the An side of the pseudoazeotrope. The thin bright edge is likely due to Na ingress from the Ba carbonate sleeve. Numbers reference the line scans in Figure 3c. (c). Variation in Na (cations/8 oxygens) through plagioclase crystals in Figure 3b. The core composition is more sodic than the bulk composition (red line) and the edges more calcic. This indicates that this composition lies on the An side of the pseudoazeotrope and that fractionation is occurring through formation of the reverse zoning. Compositional details are in Table S1 in the supporting information.

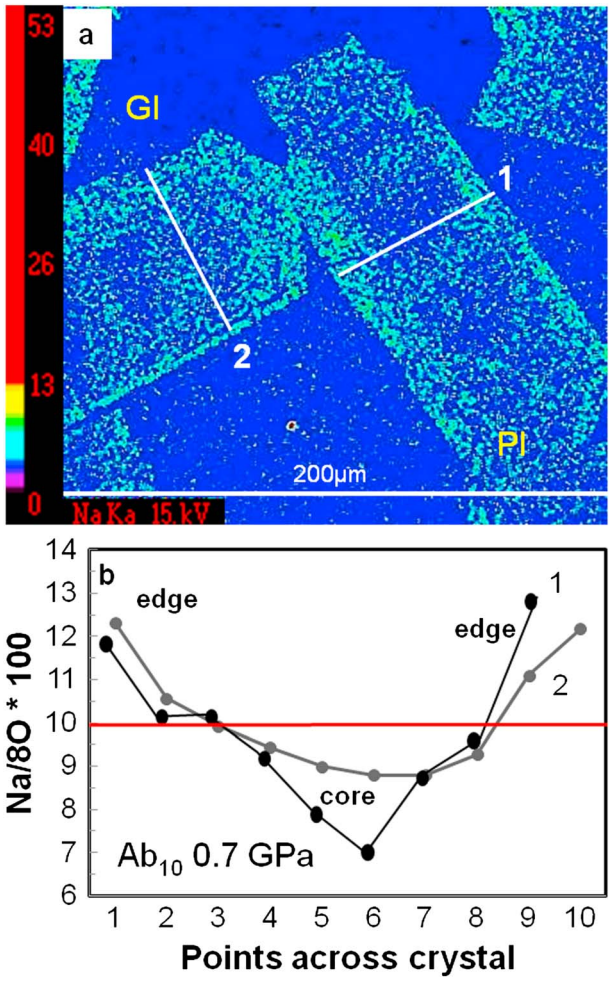

Figure 4. Characteristics of experimental products of dynamic cooling experiments at 0.7 GPa for the $(An_{90}Ab_{10})_{67}(Fo_{50}Fa_{50})_{33}$ bulk composition. (a) Na X-ray maps of characteristic plagioclase crystals from electron microprobe analysis showing plagioclase (Pl) crystals with less sodic cores than rims (normal zoning). (b) Variation in Na (cations/8 oxygens) through plagioclase crystals in Figure 4a showing cores with An content higher than the bulk composition extending to more sodic rims that go beyond the bulk composition. These results indicate that zoning successfully produced fractionation. Compositional details are in Table S2 in the supporting information.

cooling. Each experiment was quenched rapidly (1200–100°C in approximately 5 s) in order to minimize the chances of quench overgrowths. The recovered samples were affixed to glass slides for optical microscopy and electron microprobe (EMP) analysis.

3.3. Chemical Analysis of Experimental Products

Electron microprobe analysis using the Cameca SX-100 electron microprobe at the American Museum of Natural History yielded compositional data on all phases. Analyses were performed using an accelerating voltage of 15 kV, 20 nA beam current, 5 μm defocused beam diameter, and 60 s counting times. Standards used for the six elements analyzed are as follows: Si: Lake County Plagioclase; Al and Ca: Miyake Anorthite; Na: McKee Jadeite; Fe: Rockport Fayalite; and Mg: San Carlos Olivine. The precision of the EMP data was carefully assessed because the observed compositional variations are small. Repeated analyses of the same spot on an anorthite grain resulted in no measurable loss of Na; there was also no detectable Na loss during standardization. Precision of the Na values was tested by carrying out 21 analyses of the Miyake Anorthite standard; the standard error was 0.002 wt %, much smaller than the compositional differences reported for our experiments.

4. Experimental Results

All experiments produced spinel, silicate melt, and zoned crystals of plagioclase. Figures 3 and 4 show the compositional characteristics of plagioclase crystallized from bulk compositions with An_{94} and An_{90} at 0.7 GPa (~140 km depth on the Moon).

The $An_{90}Ab_{10}$-olivine composition produced plagioclase with the expected calcic cores and sodic rims, while the $An_{94}Ab_6$-olivine composition produced sodic cores with calcic exterior zones. Quantitative Na profiles (Figure 3c and data in the supporting information (SI) Table S2) show plagioclase cores from the An_{94} bulk composition that are more albitic than the starting composition and a compositional range in keeping with that of FAS plagioclase. Importantly, this reverse zoning of plagioclase did *not* require the presence of crystalline olivine, only of olivine melt components and a reaction such as reaction ((R2)), suggesting that this unique plagioclase evolution could occur even when olivine had settled out from the melt. The more sodic composition bulk shows the expected zoning profile (Figure 4b and data in SI Table S3). The dynamic crystallization experiments on the bulk composition $(An_{95}Ab_5)_{67}(Fo_{50}Fa_{50})_{33}$ at the two pressures below 0.7 GPa indicate that the pseudoazeotrope persists to pressures as low as 0.5 GPa; however, at 0.34 GPa and below, highly calcic plagioclase undergoes only Ab enrichment.

5. Relevance to LMO Residual Liquid Compositions

Does this uncommon plagioclase behavior extend to multicomponent melts derived from the LMO? Fortunately, by the stage of plagioclase cosaturation with olivine, spinel, and one or more pyroxenes, even for grossly differing proposed LMO compositions, the compositional space for residual melts becomes quite restricted [*Charlier et al*., 2015]. Thus, plagioclase forming from any of the proposed LMO compositions provides a reasonable test of whether the pseudoazeotrope extends to LMO-relevant residual liquid compositions. From their polybaric fractionation experiments simulating a crystallizing LMO starting with the *O'Neill* [1991] LMO composition, *Charlier et al*. [2015] obtained an assemblage of plagioclase + pigeonite + (minor) olivine + spinel (trace) at 0.8 GPa. At 1280°C they obtained plagioclase with composition $An_{94.6\pm0.9}$. At lower temperature (1260°C), the plagioclase was $An_{96.0\pm0.3}$, showing the An enrichment predicted by the simpler plagioclase-olivine system. In addition, the An/(Ab + An) ratio of the bulk composition used by *Charlier et al*. [2015] was higher than that of the plagioclase cores at the highest temperature investigated at this pressure. The small change in plagioclase composition was accompanied by a change in Mg′ of coexisting olivine from 0.60 to 0.53, within the range of olivine in FAS rocks (Figure 1). The slight An enrichment of plagioclase observed in these experiments is fully in keeping with the slight An enrichment observed at the rim of some FAS plagioclase crystals from Apollo 16 samples [*Nord*, 1983; *McGee*, 1993] shown in Table S3 in the SI. Although *Nord* [1983] suggested that this zonation may have been a subsolidus change, his conclusion was in part based on the assumption that Ca enrichment of plagioclase cannot occur during crystallization from a melt, in contrast to what is shown in this study.

6. Implications

Fundamentally, the presence of a pseudoazeotrope in LMO-relevant compositions explains the observation of plagioclase compositional invariance in highly calcic lunar rocks (Figure 1). However, it also provides strong support for the LMO model by indicating that FAS plagioclase could only have formed at depths >75 km, and yet this plagioclase had access to the surface to accumulate and form the early lunar crust. However, until we know how much of the globally dispersed anorthosite is of this highly anorthitic FAS variety, we cannot exclude a more local process or serial magmatism [e.g., *Longhi*, 2003; *Gross et al*., 2014]. In these regions, anorthitic plagioclase formation and flotation could have occurred over a large crystallization temperature interval during which the ferromagnesian minerals underwent major changes in Mg′, readily covering the range shown in Figure 1. The composition of this plagioclase would remain relatively constant above 94 mol % An due to the opposing effects of plagioclase and spinel fractionation. As seen experimentally, some of this plagioclase would likely have incorporated crystalline spinel during growth and where abundant, produced spinel anorthosite [e.g., *Pieters et al*., 2011] with varied Mg′s as a primary crystallization product of the LMO or smaller magma body.

As the residual LMO liquids became restricted to increasingly shallow levels, the late stage residual assemblage could start showing Ab enrichment once the pseudoazeotrope disappeared. However, at this stage, due to earlier extensive fractionation of plagioclase from the An side of the pseudoazeotrope, the residual liquid would have become highly An enriched. Ab enrichment of this at shallow levels could produce only a vanishingly small amount of residual "albitic" melt. This residual liquid is unlikely to have been the direct source of, or contributed much to, the formation of the variety of pristine non-FAS lithologies with more sodic plagioclase.

The pseudoazeotrope, however, does allow for local production of non-FAS lithologies containing plagioclase significantly more sodic than that of the FAS (e.g., potassium, rare earth element, and phosphorus (KREEP) basalts with their sodic plagioclase, $An_{85\text{-}70}$ [e.g., *Steele et al*., 1972]; Mg and alkali norites [e.g., *Shervais*, 1989]; alkali anorthosites [e.g., *Shervais and McGee*, 1999]; and "sodic" granite [e.g., *Seddio et al*., 2010], perhaps even concurrently with FAS plagioclase). Locally efficient spinel fractionation (aided perhaps by inefficient plagioclase fractionation, particularly at the early hotter stages of plagioclase crystallization) would inhibit the rise in An/(Ab + An) ratio of the liquid (by inhibiting the ability for reaction ((R2)) to proceed to the left) during cooling and perhaps shift the liquid to the Ab side of the projected pseudoazeotrope. Such liquids would contain an excess of pyroxene and silica components and evolve to the characteristics of ur-KREEP [*Warren and Wasson*, 1979]. They may have provided the more sodic signatures seen in the plagioclase of many KREEP-bearing lunar rocks. Importantly, the production of sodic residual liquid could happen locally, thereby restricting the global distribution of KREEPy rocks and could have occurred simultaneous with anorthosite formation.

Acknowledgments
This work benefitted from the careful reviews of S.A. Morse and G.J. Taylor and the image processing assistance of A.D. Rogers. Financial support was provided by the RIS^{4}E node of the NASA Solar System Exploration Research Virtual Institute (SSERVI) and NASA LASER grant NNX14AR44G (to H.N.). SSERVI Publication # 2016–005. Supporting data are included as two tables in an SI file; any additional data or sample materials may be obtained from H.N. (e-mail: Hanna.Nekvasil@stonybrook.edu).

References

Besserer, J., F. Nimmo, M. A. Wieczorek, R. C. Weber, W. S. Kiefer, P. J. McGovern, J. C. Andrews-Hanna, D. E. Smith, and M. T. Zuber (2014), GRAIL gravity constraints on the vertical and lateral density structure of the lunar crust, *Geophys. Res. Lett.*, *41*, 5771–5777, doi:10.1002/2014GL060240.

Bowen, N. L. (1913), The melting phenomena of the plagioclase feldspars, *Am. J. Sci.*, *35*, 577–59.

Charlier, B., T. L. Grove, O. Namur, and F. Holtz (2015), Crystallization of the lunar magma ocean and the primordial differentiation of the Moon, *Lunar Planet. Sci. Conf. 46th*, 1168.

Elkins-Tanton, L. T., S. Burgess, and Q.-Z. Yin (2011), The lunar magma ocean: Reconciling the solidification process with lunar petrology and geochronology, *Earth Planet. Sci. Lett.*, *304*, 326–336.

Goodrich, C. A., G. J. Taylor, K. Keil, W. V. Boynton, and D. H. Hill (1984), Petrology and chemistry of hyperferroan anorthosites and other clasts from lunar meteorite ALHA81005, *J. Geophys. Res.*, *89*, 87–94.

Gross, J., A. H. Treiman, and C. N. Mercer (2014), Lunar feldspathic meteorites: Constraints on the geology of the lunar highlands, and the origin of the lunar crust, *Earth Planet. Sci. Lett.*, *388*, 318–328.

Hawke, B. R., et al. (2003), Distribution and modes of occurrence of lunar anorthosites, *J. Geophys. Res.*, *108*(E6), 5050, doi:10.1029/2002JE001890.

Korotev, R. L., B. L. Jolliff, R. A. Zeigler, J. J. Gillis, and L. A. Haskin (2003), Feldspathic lunar meteorites and their implications for compositional remote sensing of the lunar surface and the composition of the lunar crust, *Geochim. Cosmochim. Acta*, *67*, 4895–4923.

Lindsley, D. H. (1969), Melting relations of plagioclase at high pressures, in *Origin of Anorthosite and Related Rocks*, *NYS Mus. Sci. Ser. Mem.*, vol. 18, edited by Y. A. Isachsen, pp. 39–46, State Education Department, Univ. of the State of New York, Albany, New York.

Lindstrom, M. M., and D. J. Lindstrom (1986), Lunar granulites and their precursor anorthositic norites of the early lunar crust, *Lunar Planet. Sci. Conf. 16th*, Part 2, *J. Geophys. Res.*, *91*, D263–D276.

Longhi, J. (2003), A new view of lunar ferroan anorthosites: Postmagma ocean petrogenesis, *J. Geophys. Res.*, *108*(E8), 5083, doi:10.1029/2002JE001941.

McGee, J. J. (1993), Lunar ferroan anorthosites: Mineralogy, compositional variations, and petrogenesis, *J. Geophys. Res.*, *98*, 9089–9105.

Morse, S. A. (2013), Experimental equilibrium tested by plagioclase loop widths, *J. Petrol.*, *54*, 1793–1813.

Namur, O., B. Charlier, C. Pirard, J. Hermann, J.-P. Liégeois, and J. Vander Auwera (2011), Anorthosite formation by plagioclase flotation in ferrobasalt and implications for the lunar crust, *Geochim. Cosmochim. Acta*, *75*, 4998–5018.

Nord, G. L., Jr. (1983), Compositional variation in ferroan anorthosites: Crystallization relic or subsolidus overprint?, *LPI Tech. Rep.*, *83–02*, 62–63.

O'Neill, H. S. C. (1991), The origin of the Moon and the early history of the Earth—A chemical model. Part 1: The Moon, *Geochim. Cosmochim. Acta*, *55*, 1135–1157.

Osborn, E. F., and D. B. Tait (1952), The system diopside-forsterite-anorthite, *Am. J. Sci.*, *Bowen*, 413–433.

Papike, J. J., G. W. Fowler, and C. K. Shearer (1997), Evolution of the lunar crust: SIMS study of plagioclase from ferroan anorthosites, *Geochim. Cosmochim. Acta*, *61*, 2343–2350.

Pieters, C. M., et al. (2011), Mg-spinel lithology: A new rock type on the lunar farside, *J. Geophys. Res.*, *116*, E00G08, doi:10.1029/2010JE003727.

Piskorz, D., and D. J. Stevenson (2014), The formation of pure anorthosite on the Moon, *Icarus*, *239*, 238–243.

Raedeke, L. D., and I. S. McCallum (1980), A comparison of fractionation trends in the lunar crust and the Stillwater Complex, in *Proceedings of the Conference on Lunar Highlands Crust*, *Geochim. Cosmochim. Acta, Suppl.*, vol. 12, edited by J. J. Papike and R. B. Merrill, pp. 133–153, Elsevier, New York.

Seddio, S. M., R. L. Korotev, B. L. Jolliff, and R. A. Zeigler (2010), Comparing the bulk compositions of lunar granites, with petrologic implications, *Lunar and Planet. Sci. Conf. 41st*, Abstract no. 2688.

Shervais, J. W. (1989), Highland crust at the Apollo 14 site: A review, in *Workshop on Moon in Transition: Apollo 14, KREEP, and Evolved Lunar Rocks*, *LPI Tech. Rep.*, vol. 89–03, edited by G. J. Taylor and P. H. Warren, pp. 118–127, Lunar and Planet. Inst., Houston, Tex.

Shervais, J. W., and J. J. McGee (1999), KREEP cumulates in the western lunar highlands: Ion and electron microprobe study of alkali-suite anorthosites and norites from Apollo 12 and 14, *Am. Mineral.*, *84*, 806–820.

Smith, J. V., A. T. Anderson, R. C. Newton, E. J. Olsen, and P. J. Wyllie (1970), Petrologic history of the Moon inferred from petrography, mineralogy, and petrogenesis of Apollo 11 rocks, in *Proceedings of the Apollo 11 Lunar Science Conference*, vol. 1, pp. 897–925, Pergamon Press, Oxford, U. K.

Snyder, G. A., L. A. Taylor, and C. R. Neal (1992), A chemical model for generating the sources of mare basalts: Combined equilibrium and fractional crystallization of the lunar magmasphere, *Geochim. Cosmochim. Acta*, *56*, 3809–3823.

Stebbins, J. F., and Z. Xu (1997), NMR evidence for excess non-bridging oxygen in an aluminosilicate glass, *Nature*, *390*, 60–62.

Steele, I. M., J. V. Smith, and L. Grossman (1972), Mineralogy and petrology of Apollo 15 rake samples: I. Basalts, in *The Apollo 15 Lunar Samples*, pp. 158–160, Lunar and Planet. Inst., Houston, Tex.

Warren, P. H. (1985), The magma ocean concept and lunar evolution, *Ann. Rev. Earth Planet. Sci.*, *13*, 201–240.

Warren, P. H. (1993), A concise compilation of petrologic information on possibly pristine nonmare Moon rocks, *Am. Mineral.*, *78*, 360–376.

Warren, P. H., and J. T. Wasson (1979), The origin of KREEP, *Rev. Geophys. Space Phys.*, *17*, 73–88.

Warren, P. H. (1990), Lunar anorthosites and the magma-ocean plagioclase-flotation hypothesis: Importance of FeO enrichment in the parent magma, *Am. Mineral.*, *75*, 46–58.

Whitaker, M. L., H. Nekvasil, D. H. Lindsley, and N. J. Difrancesco (2007), The role of pressure in producing compositional diversity in intraplate basaltic magmas, *J. Petrol.*, *48*, 365–393.